Life Sciences 224 (2019) 58–66

Contents lists available at ScienceDirect

Life Sciences

journal homepage: www.elsevier.com/locate/lifescie

Z-Guggulsterone attenuates glucocorticoid-induced osteoporosis through activation of Nrf2/HO-1 signaling

Yier Xu[a], Jian Guan[b], Jianyu Xu[c], Shuilin Chen[d], Guicai Sun[d,*]

[a] Laboratory of Pharmacology, Research & Development Center of Harbin Pharmaceutical Group, Harbin 150025, China
[b] Zhengzhou Orthopaedics Hospital, Zhengzhou 450015, China
[c] Department of Radiation Oncology, Tumor Hospital of Harbin Medical University, Harbin 150081, China
[d] Department of Orthopaedics, The Fourth Hospital attached to Nanchang University, Nanchang, 330003, China

ARTICLE INFO

Keywords:
Glucocorticoid-induced osteoporosis
Z-Guggulsterone
Oxidative stress
Nrf2/HO-1 signaling

ABSTRACT

Aims: The present study aims to investigate the protective effect and underlying mechanism of *Z*-Guggulsterone (Z-GS), an active component from myrrh, on glucocorticoid-induced osteoporosis (GIO).

Main methods: GIO rats were used to simulate osteoporosis in vivo while MC3T3-E1 cells were induced to osteoblast differentiation and treated with dexamethasone to simulate osteoporosis in vitro. The rats and cells were treated with *Z*-GS according to the protocol. The bone mineral density, biomechanical parameters and microstructure of GIO rats were measured with appropriate devices. Cell viability of MC3T3-E1 cells were analyzed via CCK-8 assay. Bone turnover markers and oxidative stress markers were detected by ELISA, and the expressions of Nrf2 and HO-1 were assessed by western blot. siRNA-Nrf2 and siRNA-HO-1 were transfected in MC3T3-E1 cells to knockdown the expressions of Nrf2 and HO-1.

Key findings: *Z*-GS significantly increased the body weights and bone mineral density, ameliorated the femoral biomechanical parameters and microstructure of GIO rats. *Z*-GS treatment also reversed DXM-induced changes of bone turnover markers and oxidative stress in rats and MC3T3-E1 cells. The expressions of Nrf2 and HO-1 were inhibited in the model group and treatment with *Z*-GS could markedly increase their expressions. Nrf2 or HO-1 knockdown observably abrogated the beneficial role of *Z*-GS on cells.

Significance: Our results demonstrated that *Z*-GS exerted bone protective and antioxidant stress properties through activation of Nrf2/HO-1 signaling in GIO models in vivo and in vitro. Therefore, Z-GS could be considered as a promising candidate for the treatment of GIO.

1. Introduction

Glucocorticoid-induced osteoporosis (GIO) is one of the most common forms of secondary and iatrogenic osteoporosis, which often caused by high dosage and long-term intake of dexamethasone (DEX) [1]. Since the skeletal system is the major target of glucocorticoid, one of the main side effect of glucocorticoid is osteoporosis. It was reported that about in 30–50% of patients with chronic glucocorticoid therapy could occur the GIO [2].

Previous studies found that exogenous glucocorticoid might increase oxidative stress, which was considered as the primary pathogenesis of osteoporosis [3]. Oxidative stress arose when the balance between generation of free radical and activity of intracellular antioxidants was disturbed. DEX induces oxidative stress by promoting the generation of reactive oxygen species (ROS) or inhibiting the activation of antioxidant systems [4]. Clinical research also demonstrated that there were higher oxidative stress level and lower activity of antioxidant enzymes such as glutathione peroxidase in osteoporotic patients [5]. In addition, the expressions of oxidative stress-related genes in human osteoblasts were observed to be upregulated upon exposure to DEX [6]. Increasing evidence indicated that Nrf2 (nuclear factor (erythroid-derived 2)-like 2), a key transcription factor for endogenous antioxidative enzymes, plays a central role in the protective effect against oxidative [7]. When the oxidative damage occurs, Nrf2 transfers into nucleus and regulates the downstream antioxidative protein, such as heme oxygenase 1 (HO-1), which antagonize ROS-induced oxidative stress [8].

Z-Guggulsterone (Z-GS) [4,17(20)-pregnadiene-3,16-dione], a steroid compound isolated from myrrh, has been used as an effective herbal medicine in the treatment of various conditions, such as

* Corresponding author at: Department of Orthopaedics, The Fourth Hospital attached to Nanchang University, No. 133, Guangchang South Road, Xihu District, Nanchang, Jiangxi 330003, China.
E-mail address: 13657000633@139.com (G. Sun).

https://doi.org/10.1016/j.lfs.2019.03.051
Received 29 January 2019; Received in revised form 19 March 2019; Accepted 20 March 2019
Available online 21 March 2019
0024-3205/

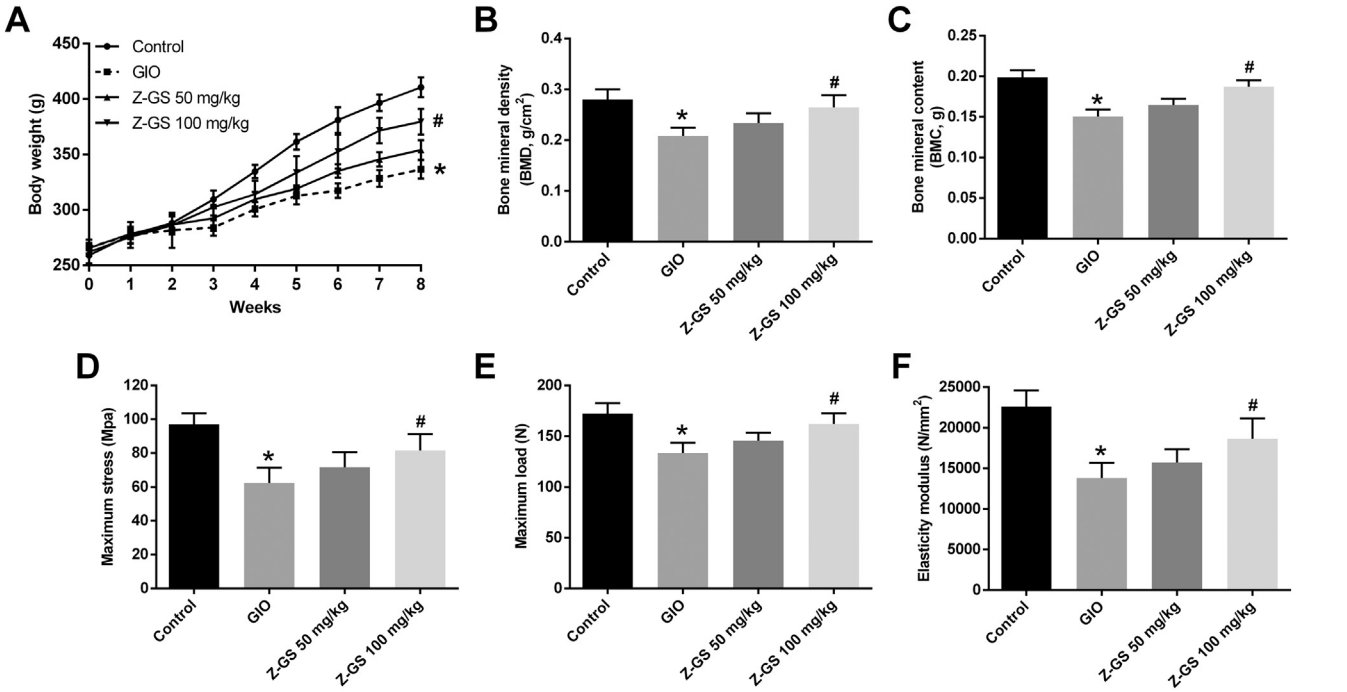

Fig. 1. Effect of Z-GS on the body weight, femoral BMD/BMC and biomechanical parameters of GIO rats. A. The body weights of the rats. B. The femoral BMD of the rats. C. The femoral BMC of the rats. D. The maximum stress of femurs. E. The maximum load of femurs. F. The elasticity modulus of femurs. Data were presented as the mean ± SD, * $p < 0.05$ versus control group; $^{\#}$ $p < 0.05$ versus GIO group.

atherosclerosis, neuroinflammation, arthritis, and cancers [9]. Accumulating evidence indicates that Z-GS possesses potential antioxidant stress by reducing the formation of intracellular ROS and MDA [10,11]. Moreover, it was reported that Guggulsterone (GS) treatment enhanced nuclear translocation of Nrf2 and expression of HO-1 in human mammary epithelial cells [12]. However, it is unknown whether the protective potentiality of *Z*-GS is applicable in protecting against GIO. Based on the evidences above, we aim at exploring the protective effect and mechanism of Z-GS in GIO rats and MC3T3-E1 cells.

2. Results

2.1. Effect of Z-GS on the body and bone weights of GIO rats

The body weights of the rats were measured weekly throughout the experimental period. As shown in Fig. 1A, there were no differences in the initial weights of the four groups. The body weights in control group were increased gradually while increased slowly in GIO group, and the differences between the two groups were statistically significant from the fourth week. As expected, the treatment of *Z*-GS (100 mg/kg) significantly increased body weights as compared with the GIO group. In addition, the femoral weight and length were measured using an electronic scale and a vernier caliper. However, there's no significant difference among the groups (data not shown).

2.2. Effect of Z-GS on the femoral BMD and BMC of GIO rats

Bone mineral density (BMD) and bone mineral content (BMC) are important indicators in osteoporosis. In this study, femoral BMD were significantly decreased in the GIO rats. Treatment with *Z*-GS at the dose of 50 and 100 mg/kg partly recovered the loss of BMD. And high dosage group has significant improvement compared to the GIO group (Fig. 1B). The same effects were also observed in BMC (Fig. 1C).

2.3. Effect of Z-GS on the femoral biomechanical parameters of GIO rats

The biomechanical parameters of femurs were measured using the three-point bending test. The results showed that the maximum stress, maximum load and elasticity modulus were lower in the GIO group. However, 100 mg/kg of Z-GS treatment significantly increased these parameters (Fig. 1D–F).

2.4. Effect of Z-GS on the femoral microstructure of GIO rats

The micro-CT was used to analyze the trabecular parameters, including bone volume/tissue volume (BV/TV), trabecular thickness (Tb.Th), trabecular separation (Tb.Sp), and trabecular number (Tb.N). The results (Fig. 2) showed that DXM significantly decreased BV/TV, Tb.Th and Tb.N while increased Tb.Sp of the rats' femoral region. Treatment with *Z*-GS, however, reversed these changes in the GIO rats.

2.5. Effect of Z-GS on the ratio of RANKL/OPG expression in GIO rats

The RANKL/OPG ratio is a key value to monitor the balance of bone resorption and formation. Western blot suggested that DXM induced a significant overexpression of RANKL and low expression of OPG. The elevated ratio of RANKL/OPG expression was alleviated by *Z*-GS treatment (Fig. 2E).

2.6. Effect of Z-GS on the bone turnover markers of GIO rats

Bone turnover markers, including alkaline phosphatase (ALP), tartrate-resistant acid phosphatase (TRAP), osteocalcin (OCN) and carboxy-terminal telopeptide of type 1 collagen (CTX-I), were detected from the serum of the rats. Results indicated that the level of ALP, TRAP and CTX-I were significantly increased in the GIO rats while OCN level was decreased. The treatment of *Z*-GS reversed the changes of these markers. In addition, *Z*-GS markedly counteracted DEX-induced downregulation of Runx2 and BMP2 expressions (Fig. 3).

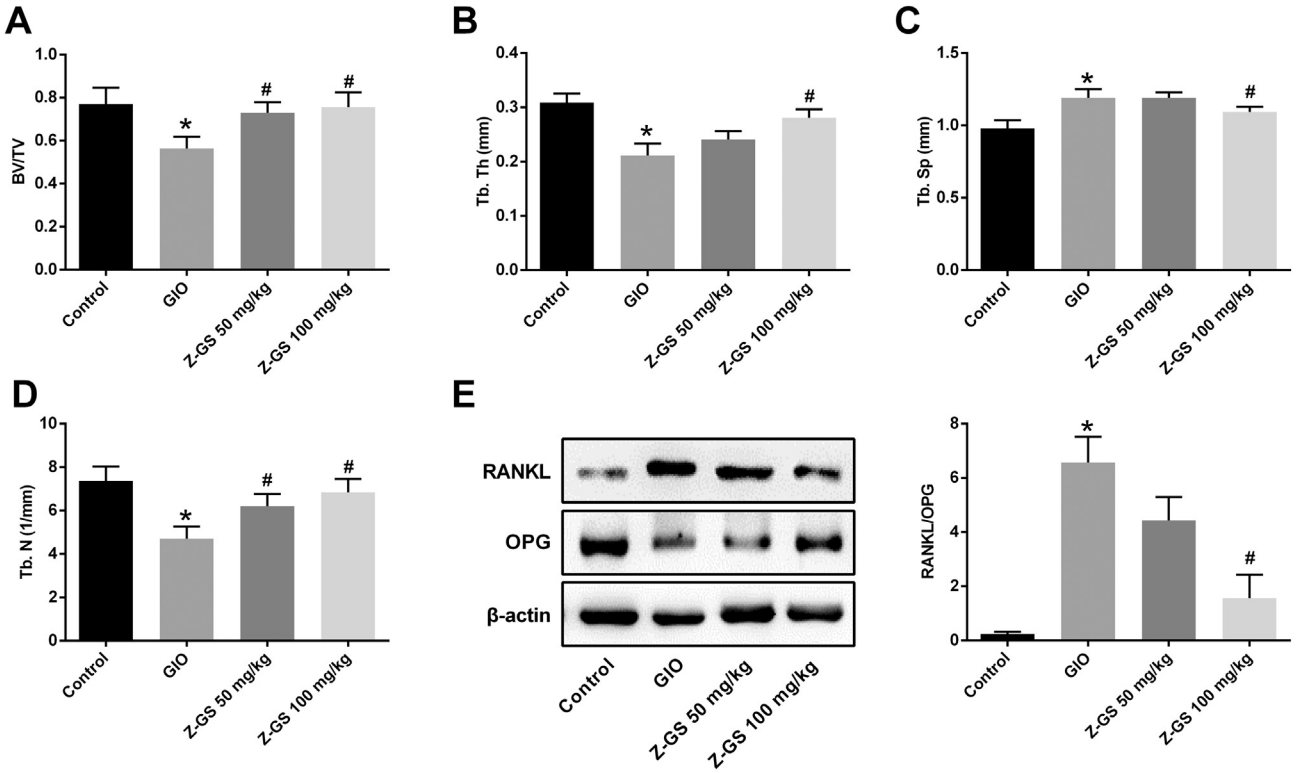

Fig. 2. Effect of *Z*-GS on the femoral microstructure and RANKL/OPG ratio of GIO rats. A. The bone volume/tissue volume (BV/TV) of femurs. B. The trabecular thickness (Tb.Th) of femurs. C. The trabecular separation (Tb.Sp) of femurs. D. The trabecular number (Tb.N) of femurs. E. The protein expressions of RANKL and OPG in femurs tissues. Data were presented as the mean ± SD, * $p < 0.05$ versus control group; $^{\#}$ $p < 0.05$ versus GIO group.

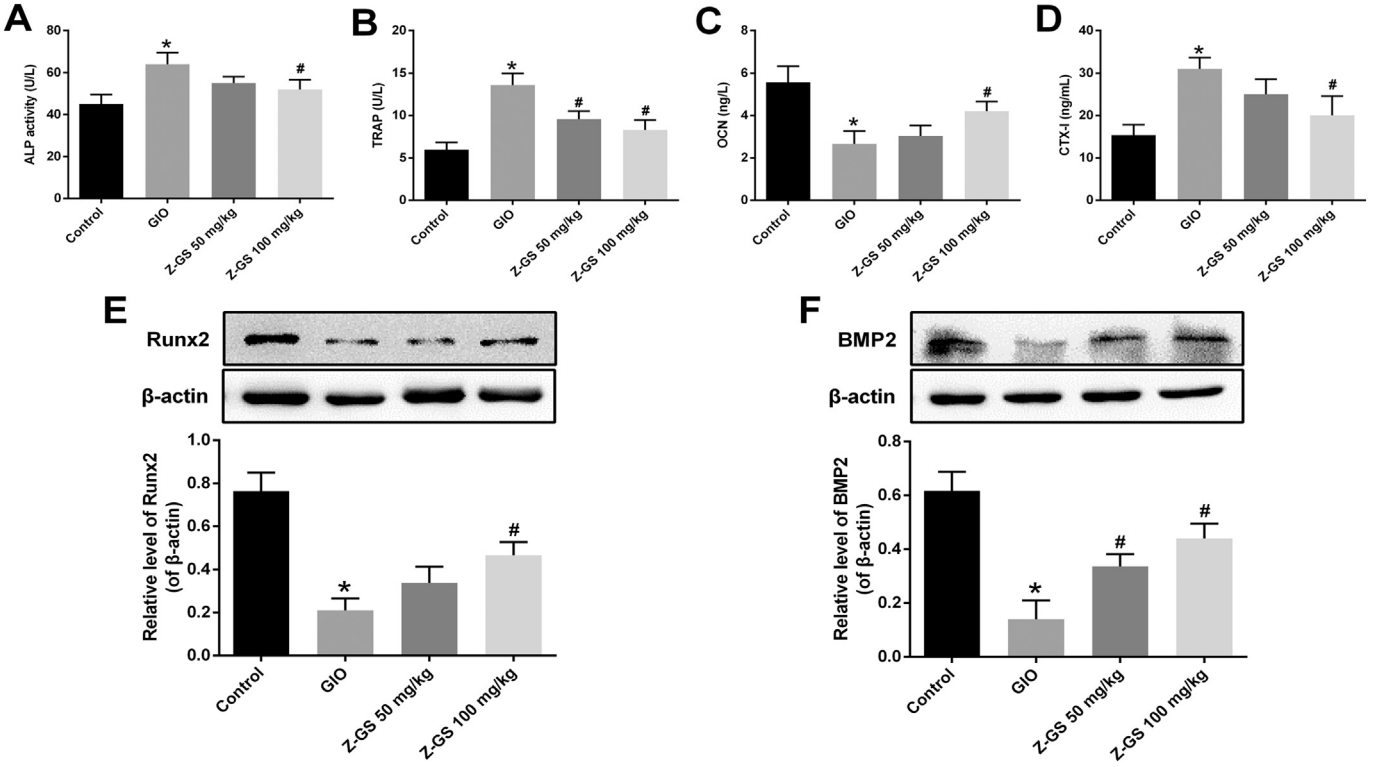

Fig. 3. Effect of Z-GS on the bone turnover markers of GIO rats. A. The serum ALP activity. B. The serum TRAP activity. C. The serum OCN content. D. The serum CTX-I content. E. The protein expression of Runx2 in femurs tissues. F. The protein expression of BMP2 in femurs tissues. Data were presented as the mean ± SD, * $p < 0.05$ versus control group; $^{\#}$ $p < 0.05$ versus GIO group.

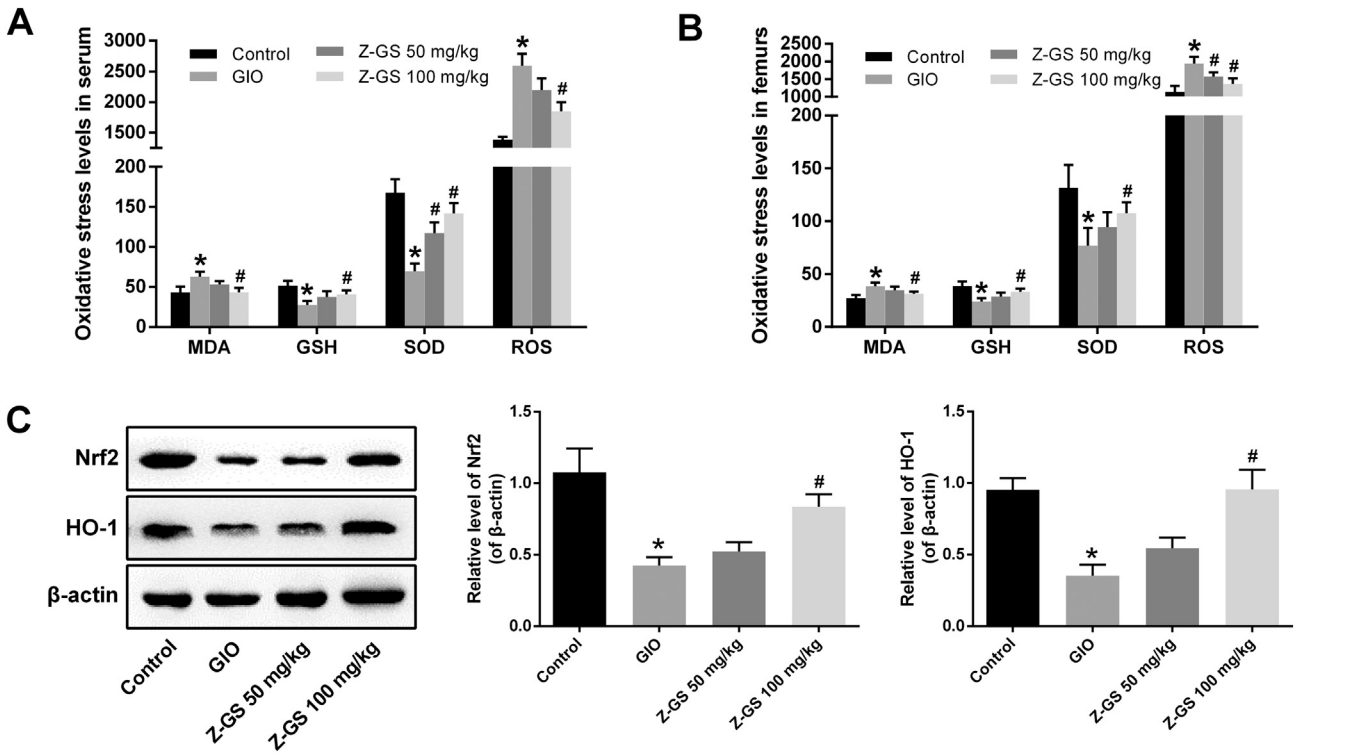

Fig. 4. Effect of Z-GS on the oxidative stress level of GIO rats. A. The oxidative stress levels in rat's serum, including MDA (μmol/ml), GSH (μmol/ml), SOD (U/ml) and ROS (U/ml). B. The oxidative stress level in rat's femurs, including MDA (nmol/mg), GSH (nmol/mg), SOD (mU/mg) and ROS (mU/mg). C. The protein expressions of Nrf2 and HO-1 in femurs tissues. Data were presented as the mean ± SD, $^{*}p < 0.05$ versus control group; $^{\#}p < 0.05$ versus GIO group.

2.7. Effect of Z-GS on the oxidative stress level of GIO rats

Oxidative stress level in rat's serum and femurs were investigated. The results showed that the malondialdehyde (MDA) and ROS levels in serum and femurs were increased in the GIO rats compared with the control, and Z-GS treatment markedly decreased MDA and ROS contents. The glutathione (GSH) level and superoxide dismutase (SOD) activity were decreased in the GIO rats compared with the control group, and treatment with *Z*-GS upregulated their levels (Fig. 4A, B).

2.8. Effect of Z-GS on the Nrf2/HO-1 pathway of GIO rats

The classical oxidative stress pathway was examined to reveal the possible mechanism. As shown in Fig. 4C, the protein expressions of Nrf2 and HO-1 were inhibited in the GIO group and treatment with *Z*-GS could markedly increase their expressions in the femur of the rats.

2.9. Effect of Z-GS on the cell function and oxidative stress in MC3T3-E1 cells

As shown in Fig. 5A, DXM decreased osteoblast cell viability and increased the LDH level, whereas treatment with *Z*-GS reversed the DXM-induced changes in cell viability and LDH, indicating the protective effect of Z-GS on MC3T3-E1 cells.

To validate the antioxidant effect of Z-GS, the ROS accumulation were detected. The results revealed that DXM increased ROS accumulation both in intracellular and mitochondrial. In contrast, treatment with Z-GS inhibited the increase of ROS levels (Fig. 5B). In addition, we detected the antioxidant enzyme activity in MC3T3-E1 cells, the results indicated that *Z*-GS could significantly promote the activities of SOD and GSH in osteoblasts (Fig. 5C).

2.10. Effect of Z-GS on the bone turnover markers in MC3T3-E1 cells

Bone turnover markers in MC3T3-E1 cells were further detected to test the repair function of *Z*-GS on osteoporosis. The ELISA results showed that DXM increased the levels of ALP and TRAP in MC3T3-E1 cells, while Z-GS treatment inhibited these changes (Fig. 5D). Moreover, the reduced expressions of Runx2 and BMP2 induced by DXM were also observably reversed by *Z*-GS (Fig. 5E).

2.11. Nrf2/HO-1 knockdown abrogated the beneficial role of Z-GS in DXM-treated MC3T3-E1 cells

To further determine the role of Nrf2/HO-1 signaling in the beneficial effects of Z-GS, Nrf-2 and HO-1 were thus silenced in the cultured MC3T3-E1 cells through transfecting with siRNA-Nrf2 or siRNA-HO-1. The transfection efficiency was confirmed by western blotting (Figs. 6A, 7A). The results indicated that Nrf2 knockdown largely inhibited the expression of HO-1 (Fig. 6B). Besides, the effects of Z-GS on the expressions of bone markers, Runx2 and BMP2, in DXM-treated MC3T3-E1 cells were also greatly weakened by Nrf2 knockdown (Fig. 6C). The similar results were found in siRNA-HO-1 transfected cells (Fig. 7).

3. Discussion

Osteoporosis is a disease with high risk of bone fragility and fracture, which is the major reason for broken bone in the elderly population [13]. Epidemiologic investigations have accumulatively identified that glucocorticoid contributes to the incidence of secondary osteoporosis [14]. Ample evidence has demonstrated that oxidative stress induced osteoblast injure is one of the vital pathological mechanisms of GIO, and the antioxidants could be used to treat or prevent GIO [15]. *Z*-GS is the major component of myrrh and is believed to have a considerable antioxidative potential. In our study, we aimed to get full use of the natural bioactive component Z-GS and evaluate it as a novel

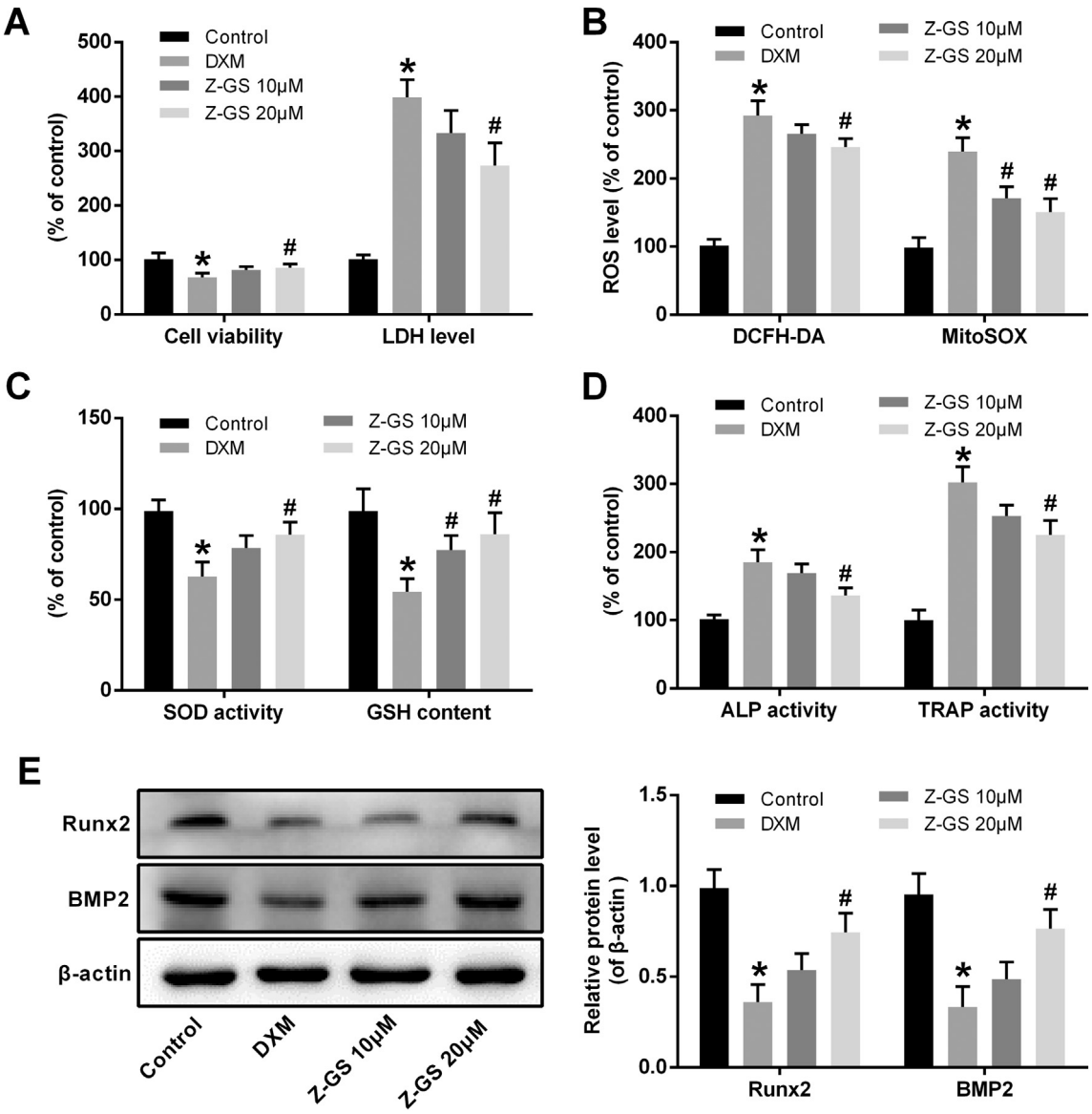

Fig. 5. Effect of *Z*-GS on the oxidative stress and bone markers in MC3T3-E1 cells. A. The cell viability and LDH level of MC3T3-E1 cells. B. The ROS levels in intracellular and mitochondrial. C. The SOD and GSH content in MC3T3-E1 cells. D. The ALP and TRAP activity in MC3T3-E1 cells. E. The protein expressions of Runx2 and BMP2 in MC3T3-E1 cells. Data were presented as the mean ± SD, $^{*}p < 0.05$ versus control group; $^{\#}p < 0.05$ versus DXM group.

pharmacological agent for GIO. Rats were injected with DXM for 8 weeks to establish the GIO model in vivo, meanwhile MC3T3-E1 cells were incubated with DXM to mimic the GIO model in vitro.

BMD and BMC were gold standards of osteoporosis diagnosis, which could be determined by DEXA assay [16]. We found that Z-GS treatment significantly increased the levels of BMD and BMC in the GIO rats. Moreover, we used three-point bending test to analyze bone biomechanical parameters of femurs. The results indicated that DXM induced the decrease of maximum stress, maximum load and elasticity modulus, while treatment with *Z*-GS reversed these parameters. In addition, the micro-CT analysis showed that DXM caused severely damage to the microarchitecture of femur and *Z*-GS successfully prevented the destructive effect of DXM. These results suggested that Z-GS could enhance bone mass and strength of GIO rats.

RANKL and its decoy receptor OPG were essential factors that regulate the balance between bone formation and resorption in GIO [17]. RANKL can ligate to its receptor RANK and then initiate bone resorption by increasing osteoclastic activities. Conversely, the OPG could prevent the interaction of RANKL-RANK and inhibit bone resorption [18]. Therefore, the increased expression of the RANKL or RANKL/OPG ratio could alter bone homeostasis and finally lead to osteoporosis [19,20]. In our study, it was interestingly noted that DXM induced a significant overexpression of RANKL rather than OPG in GIO rats. The enhanced RANKL/OPG ratio were alleviated in *Z*-GS-treated rats, potentially explaining the protective effect of Z-GS on GIO.

To further investigate the role of Z-GS in bone formation and bone resorption, several bone turnover markers, including ALP, TRAP, OCN, CTX-I, Runx2 and BMP2 were determined. ALP is a vital marker in the early stage of osteogenic differentiation, the level of ALP is higher in the osteoporosis patients and is negatively correlated with BMD [21]. TRAP is a mediator of osteoclast differentiation, which is usually overexpressed in osteoclasts [22]. OCN is a late differentiation marker and CTX-I is a product of collagen I and commonly used as a bone resorption marker [23]. In accordance with previous studies [4], our results revealed that DXM resulted in the decrease OCN level as well as the increase of ALP and TRAP activities and CTX-I level. However, *Z*-GS finally ameliorated the damages induced by DXM.

BMP2/Runx2 cascade is also the key mediator in the osteogenic

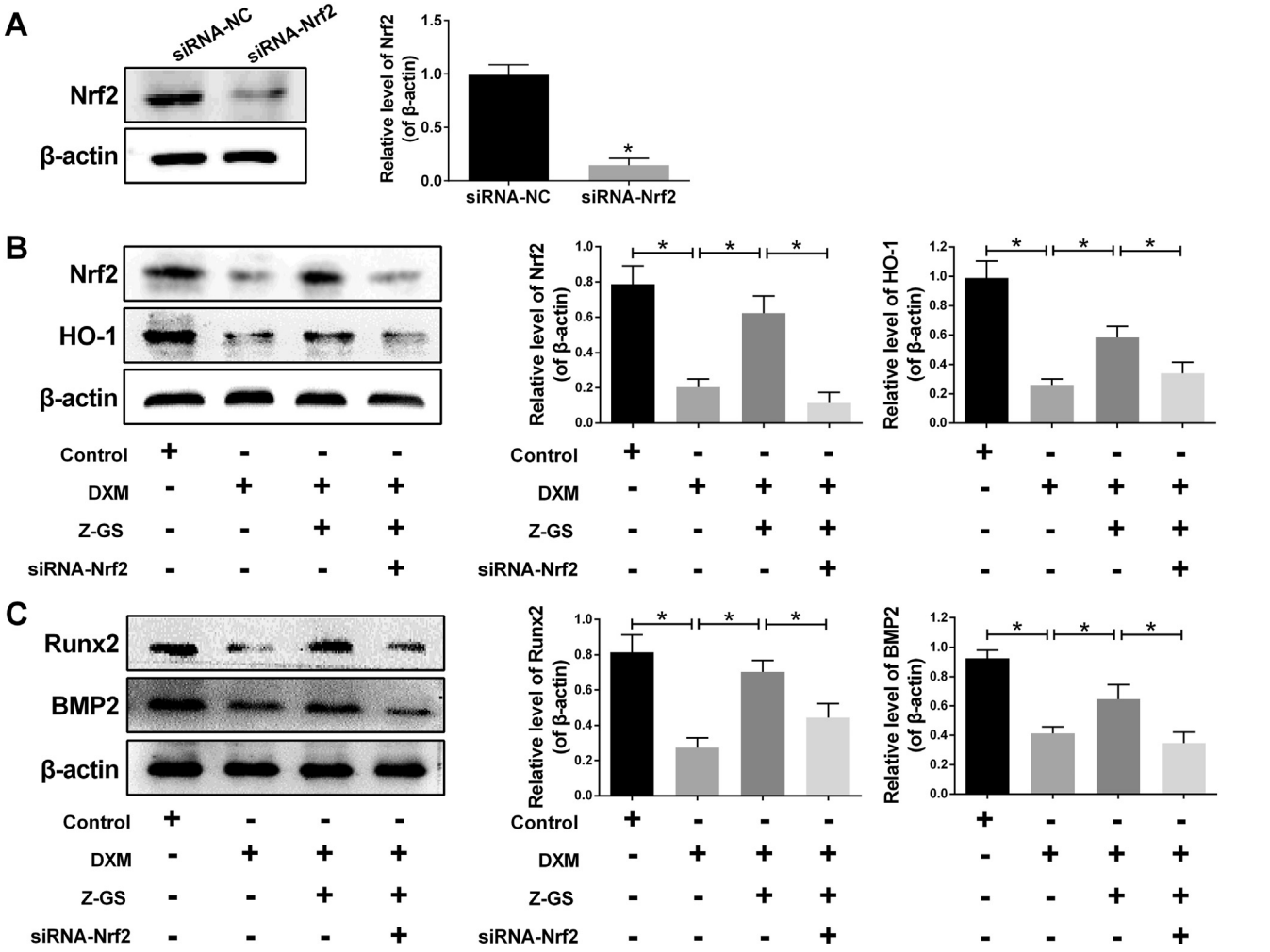

Fig. 6. Nrf2 knockdown abrogated the beneficial role of *Z*-GS in DXM-treated MC3T3-E1 cells. A. The transfection efficiency of siRNA-Nrf2 was confirmed by western blotting. B. The protein expressions of Nrf2 and HO-1 in siRNA-Nrf2 transfected MC3T3-E1 cells. C. The protein expressions of Runx2 and BMP2 in siRNA-Nrf2 transfected MC3T3-E1 cells. * $p < 0.05$ between the two groups.

differentiation. BMP2 is a growth factor that can promote osteogenic differentiation via activating the downstream transcriptional factors, including Runx2 [24]. Then Runx2 binds to the promoters of osteogenic genes and thus regulates the expressions of bone turnover markers [25]. In the present study, treatment of *Z*-GS reversed the reduction of BMP2 and Runx2 expression in GIO rats.

To investigate the potential mechanism of Z-GS on GIO rats, we detected the varying of oxidative stress level in vivo and in vitro. MDA is one of the important products of peroxidation, it indicates the level of oxidative stress in body. SOD and GSH are two critical antioxidant enzymes in cells, they can resist and repair the damage caused by oxygen free radicals [26]. Our results indicated that *Z*-GS could significantly reduce the MDA level and enhance GSH and SOD activities in GIO rats. Similar findings were observed in Z-GS treated MC3T3-E1 cells.

It is generally accepted that ROS contributes to the destruction of cellular components in various pathological conditions, including osteoporosis [27]. Researches have revealed that glucocorticoid could initiate the generation of ROS, and most of them were derived from mitochondria [28]. Hence, we analyzed the cellular and mitochondrial ROS production in MC3T3-E1 cells, and the results indicated that *Z*-GS treatment inhibited the level of ROS. All these findings suggested that antioxidative stress is the possible mechanism of *Z*-GS on GIO rats.

The Nrf2 pathway constitutes one of the major cellular defense mechanisms against oxidative stress [29]. Nrf2 offer cytoprotection through binding to antioxidant responsive element (ARE) and enhancing the expression of antioxidants, such as HO-1 [30]. Emerging studies have suggested that Nrf2 signaling pathway played a critical role in the regulation of bone metabolism [31]. Deletion of Nrf2 could inhibit the activity of antioxidant enzymes and elevate the level of ROS in osteoclasts [32,33]. Consistent with these previous evidences, the protein expressions of Nrf2 and HO-1 in the present study were suppressed in DXM induced femurs and cells and *Z*-GS treatment promoted their expressions.

To confirm the pivotal role of Nrf2/HO-1 pathway in the antioxidative stress effect of Z-GS, Nrf2 and HO-1 siRNA were employed to down regulate their expressions. The results showed that Nrf2 and HO-1 were significantly suppressed by using specific Nrf2 and HO-1 siRNA. Moreover, the beneficial effects of Z-GS on HO-1 and Runx2 as well as BMP2 were reversed by siRNA-Nrf2 or siRNA-HO-1. These results suggested that the antioxidative stress effects of Z-GS is mediated by the activation of Nrf2/HO-1 pathway.

Taken together, these findings demonstrated that Z-GS inhibited the oxidative stress injury to ameliorate the bone destruction in GIO rats through activating Nrf2/HO-1 pathway. *Z*-GS could be a promising candidate agent for the treatment of GIO.

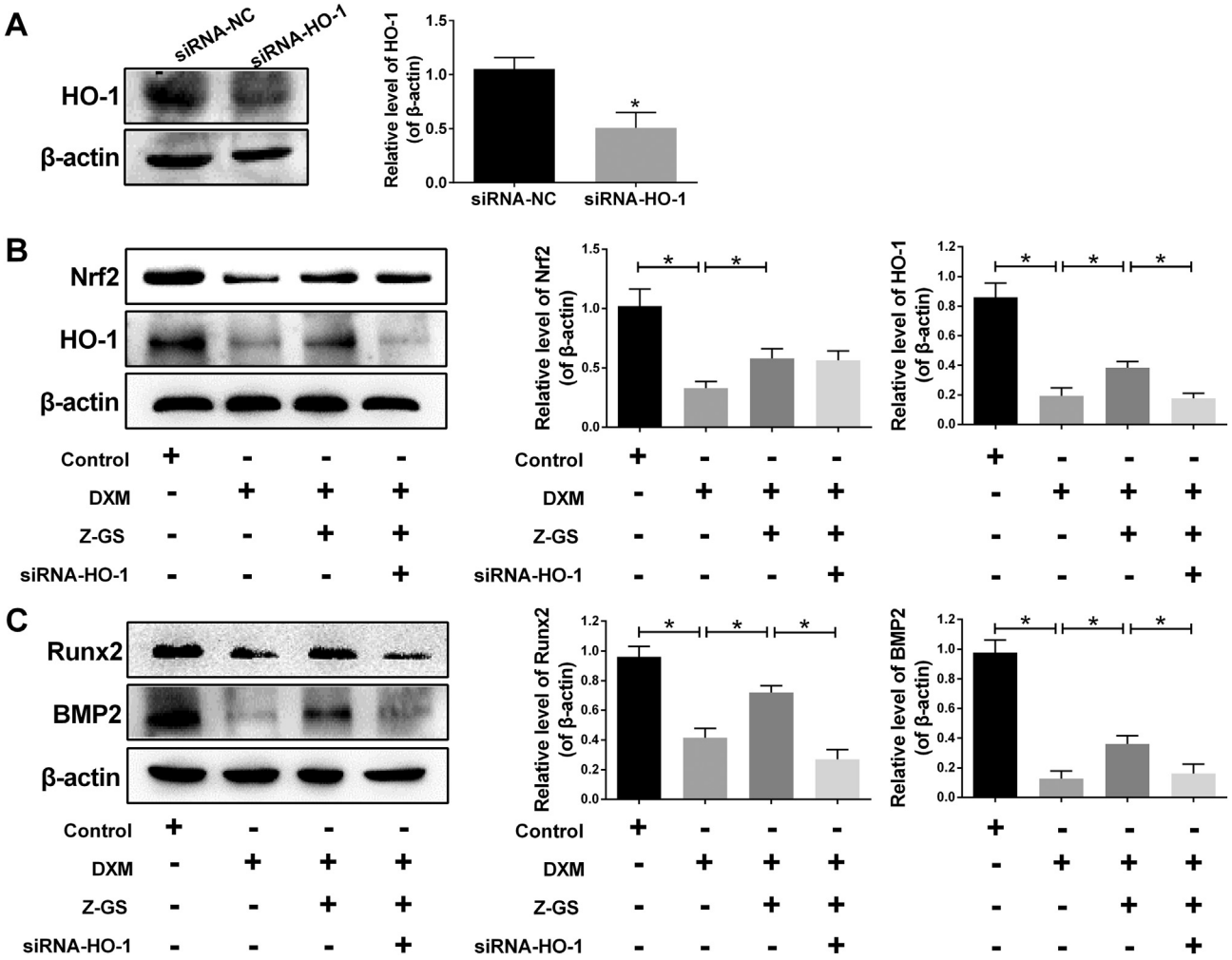

Fig. 7. HO-1 knockdown abrogated the beneficial role of *Z*-GS in DXM-treated MC3T3-E1 cells. A. The transfection efficiency of siRNA-HO-1 was confirmed by western blotting. B. The protein expressions of Nrf2 and HO-1 in siRNA-Nrf2 transfected MC3T3-E1 cells. C. The protein expressions of Runx2 and BMP2 in siRNA-HO-1 transfected MC3T3-E1 cells. * $p < 0.05$ between the two groups.

4. Materials and methods

4.1. Reagents

Z-Guggulsterone (MF: $C_{21}H_{28}O_2$, CAS: 39025-23-5, purity: > 98%) was purchased from R&D Systems (Minnesota, USA), dexamethasone (MF: $C_{22}H_{29}FO_5$, CAS: 50-02-2, purity: > 98%) was purchased from ACMEC (Shanghai, China).

4.2. GIO model and administration

The animal experiment was approved by Ethical Review Committee of University, and was conducted following the ARRIVE guidelines and the National Institutes of Health guide for the care and use of Laboratory animals. Thirty-two 8-week old SPF female SD rats (weighing 250 ± 10 g) were purchased from Beijing HFK Bioscience Co., Ltd. All the rats were housed in air-conditioned animal quarters in a constant 12-hour light/dark cycle at 25 ± 2 °C temperature and 50 ± 10% air humidity with free access to pellet food and water. After 7 days of acclimatization, the rats were randomly divided into four groups (n = 8): control group, GIO model group, *Z*-GS 50 mg/kg group and Z-GS 100 mg/kg group. The GIO model was established by the intramuscular injection of 2.5 mg/kg DXM, twice per week for two months. The rats in the Z-GS treatment groups were intraperitoneally injected with 50 or 100 mg/kg Z-GS (dissolved in soybean oil solvent) once a day for two months. The rats in control and GIO groups were received equivalent soybean oil solvent. Body weight was measured once a week for eight weeks. The rats were euthanized, and their serum and femurs were collected after two months of administration.

4.3. Bone mineral density and biomechanics measurements

BMD and BMC were measured by dual-energy X-ray absorptiometry (DEXA) with a PIXImus II densitometer (GE Medical Systems, Lunar Division, Madison, United States) on the proximal area of left femurs.

Bone biomechanical testing was conducted by a computer-controlled mechanical testing machine (SANS-10404043, Shenzhen, China). The maximum bending stress, maximum load and elasticity modulus were detected according to the three-point bend testing. The texting conditions were: sample space = 23 mm and plunger speed = 2.0 mm/min at room temperature.

4.4. Bone microstructure measurements

Bone microstructure were scanned by a micro-computed tomography (micro-CT; QuantumGX, PerkinElmer, United States), the parameters were assessed within the same regions of interest in cross section of the left femur. The structural parameters including BV/TV, Tb.N, Tb.Th and Tb.Sp. The scan conditions: source voltage of 90 kV, source current of 88 mA, exposure time of 14 s, and resolution of 2 mm.

4.5. Mineral and biochemistry analysis in serum and cells

The levels of ALP, TRAP, OCN and CTX-I in serum and MC3T3-E1 cells were analyzed by commercially available assay kits (Nanjing Jiancheng, Nanjing, China) according to the manufacturer's instructions.

4.6. Cell culture and treatment

MC3T3-E1 cells were obtained from the American Type Culture Collection (Manassas, VA, USA). Cells were cultured in Dulbecco's modified Eagle's medium (DMEM; Gibco, Grand Island, NY, USA) supplemented with 10% fetal bovine serum (FBS, Gibco) at 37 °C in a 5% CO_2 humidified cell incubator. To induce osteogenic differentiation, MC3T3-E1 cells were cultured in DMEM with 10 mM β-glycerophosphate and 50 mg/L ascorbic acid. The induced MC3T3-E1 cells were treated with 100 μM DXM in the presence or absence of *Z*-GS (10 and 20 μM) for 7 days.

4.7. Small interfering RNA transfection

To knock down the expression of Nrf2 or HO-1, 1×10^6 MC3T3-E1 cells were transfected with siRNA-Nrf2, siRNA-HO-1 or siRNA-Negative control (siRNA-NC), which were purchased from GenePharma Co., Ltd. (Shanghai, China). Transient siRNA transfection was performed with Lipofectamine 3000 (Invitrogen) reagent according to the manufacturer's instructions. After 24 h of transfection, the cells were treated with DXM and different concentrations of Z-GS. The transfection efficiency was confirmed by western blotting.

4.8. Cell viability and toxicity assay

The CCK-8 assay was carried out for measuring cell viability. Briefly, MC3T3-E1 cells were seeded at a density of 5×10^3 cells/well in 96-well plates, after the DXM and Z-GS treatment, 10 mL of CCK-8 reagent was added to each well and incubation was continued for 2 h. Absorbance was read at 450 nm on a microplate reader to determine cell viability. The cell toxicity was detected by a cellular lactate dehydrogenase (LDH) assay kit (Nanjing Jiancheng, Nanjing, China) according to the manufacturer's instructions.

4.9. Oxidative stress detection

The oxidative stress activity in serum, femurs and MC3T3-E1 cells were estimated by GSH, MDA and SOD assay kits (Nanjing Jiancheng, Nanjing, China) according to the manufacturer's instructions. The ROS levels in serum and femurs tissues were detected by a ROS ELISA kit (Lianshuo Biological Technology, Shanghai, China) following the protocol. The intracellular and mitochondrial ROS in MC3T3-E1 cells were evaluated by DCFH-DA probe (10 mM) and MitoSOXTM Red florescent probe (5 mM), respectively. The fluorescence intensity was detected by FACScan flow cytometry (Becton Dickinson, Franklin Lakes, NJ, United States).

4.10. Western blotting

Femurs tissues or cells were homogenized in RIPA buffer (Beyotime, Shanghai, China). The protein concentration was determined using a Bicinchoninic acid (BCA) protein assay kit (Beyotime). Protein samples were separated with 12% SDS-PAGE gels and then transferred onto polyvinylidenedifluoride (PVDF) membranes (Bio-Rad, Hercules, CA, USA). The membranes were blocked with 5% nonfat milk and incubated with specific antibodies: anti-Nrf2 (1:500, Abcam), anti-HO-1 (1:1000, CST), anti-OPG (1:1000, CST), anti-RANKL (1:1000, Abcam), anti-Runx2 (1:1000, Abcam), and anti-BMP2 (1:1000, Abcam) overnight at 4 °C. Membranes were incubated with anti-rabbit IgG or anti-mouse IgG secondary antibodies (1:2000; ZSGB-Bio, Beijing, China) at 37 °C for 2 h. β-actin was used as an internal control. Protein bands were visualized by enhanced chemiluminescent (ECL) reagents (Beyotime) and analyzed by Image J software.

4.11. Statistical analysis

Data were expressed as means ± SD. Difference among groups were analyzed by one-way analysis of variance (ANOVA) followed by Tukey test using GraphPad Prism version 6 (GraphPad Software, Inc., La Jolla, CA, USA). $p < 0.05$ was considered statistically significant.

Abbreviations

BMC	Bone mineral content
BMD	Bone mineral density
DEX	Dexamethasone
GIO	Glucocorticoid-induced osteoporosis
ROS	Reactive oxygen species
Z-GS	Z-Guggulsterone

Conflict of interest statement

The authors declare that there are no conflicts of interest.

Acknowledgments

This work was funded by the National Natural Science Foundation of China (No. 81660801).

References

[1] L. Buckley, M. Humphrey, Glucocorticoid-induced osteoporosis, N. Engl. J. Med. (26) (2018) 2547–2556.
[2] T. Komori, Glucocorticoid signaling and bone biology, Horm. Metab. Res. 11 (2016) 755–763.
[3] Q Z., L Z., D Z., N L., Q L., P D., Y M., X L., J M., S H., Oxidative stress-related biomarkers in postmenopausal osteoporosis: a systematic review and meta-analyses, Dis. Markers 2016 (2016) 1–12.
[4] Z. Jing, C. Wang, Q. Yang, X. Wei, Y. Jin, Q. Meng, Q. Liu, Z. Liu, X. Ma, K. Liu, et al., Luteolin attenuates glucocorticoid-induced osteoporosis by regulating ERK/Lrp-5/GSK-3β signaling pathway in vivo and in vitro, J. Cell. Physiol. (4) (2019) 4472–4490.
[5] P. V, J. Z., V M., T. K., J. M., B K., B. O, Epigenetic enzymes influenced by oxidative stress and hypoxia mimetic in osteoblasts are differentially expressed in patients with osteoporosis and osteoarthritis, Sci Rep-UK 1 (2018) 16215.
[6] S. Liu, L. Yang, S. Mu, Q. Fu, Epigallocatechin-3-gallate ameliorates glucocorticoid-induced osteoporosis of rats in vivo and in vitro, Front. Pharmacol. 9 (2018) 447.
[7] W.A. Ahmad, H. Zeenat, B.S. Ahmad, S.N.U. Din, B. Musadiq, Relaxin protects cardiomyocytes against hypoxia-induced damage in in-vitro conditions: involvement of Nrf2/HO-1 signaling pathway, Life Sci. 213 (2018) 25–31.
[8] G. Zu, T. Zhou, N. Che, X. Zhang, Salvianolic acid a protects against oxidative stress and apoptosis induced by intestinal ischemia-reperfusion injury through activation of Nrf2/HO-1 pathways, Cell. Physiol. Biochem. 49 (2018) 2320–2332.
[9] T. Liu, M. Liu, T. Zhang, W. Liu, H. Xu, F. Mu, D. Ren, N. Jia, Z. Li, Y. Ding, et al., Z-Guggulsterone attenuates astrocytes-mediated neuroinflammation after ischemia by inhibiting toll-like receptor 4 pathway, J. Neurochem. 147 (2018) 803–815.
[10] W. Wang, Y. Uen, M. Chang, K. Cheah, J. Li, W. Yu, K. Lee, C. Choy, C. Hu, Protective effect of guggulsterone against cardiomyocyte injury induced by doxorubicin in vitro, BMC Complement. Altern. Med. 12 (2012) 138.
[11] H.B. Xu, L. Li, G.Q. Liu, Protection against hydrogen peroxide-induced cytotoxicity in PC12 cells by guggulsterone, Yao Xue Xue Bao 43 (2008) 1190–1197.
[12] I. Almazari, J.M. Park, S.A. Park, J.Y. Suh, H.K. Na, Y.N. Cha, Y.J. Surh, Guggulsterone induces heme oxygenase-1 expression through activation of Nrf2 in human mammary epithelial cells: PTEN as a putative target, Carcinogenesis 33 (2012) 368–376.
[13] M. Carter, Prevention of glucocorticoid-induced osteoporosis: clinical audit to evaluate the implementation of National Osteoporosis Guideline Group 2017 guidelines in a primary care setting, J. Clin. Densitom. 22 (2019) 25–30.
[14] J. Compston, Glucocorticoid-induced osteoporosis: an update, Endocrine 61 (2018) 7–16.
[15] T. Wang, C. Han, P. Tian, P.F. Li, X.L. Ma, Role of teriparatide in glucocorticoid-induced osteoporosis through regulating cellular reactive oxygen species, Orthop. Surg. (2) (2018) 152–159.
[16] J. Valente-Dos-Santos, Ó.M. Tavares, J.P. Duarte, P.M. Sousa-E-Silva, L.M. Rama, J.M. Casanova, C.A. Fontes-Ribeiro, E.A. Marques, D. Courteix, E.R.V. Ronque,

Total and regional bone mineral and tissue composition in female adolescent athletes: comparison between volleyball players and swimmers, BMC Pediatr. 18 (2018) 212.
[17] N. Kondegowda, R. Fenutria, I. Pollack, M. Orthofer, A. Garcia-Ocaña, J. Penninger, R. Vasavada, Osteoprotegerin and denosumab stimulate human Beta cell proliferation through inhibition of the receptor activator of NF-κB ligand pathway, Cell Metab. 22 (2015) 77–85.
[18] E. Harper, H. Forde, C. Davenport, K.D. Rochfort, D. Smith, P.M. Cummins, Vascular calcification in type-2 diabetes and cardiovascular disease: integrative roles for OPG, RANKL and TRAIL, Vasc. Pharmacol. 82 (2016) 30–40.
[19] Y. Yin, L. Tang, J. Chen, X. Lu, MiR-30a attenuates osteoclastogenesis via targeting DC-STAMP-c-Fos-NFATc1 signaling, Am. J. Transl. Res. 9 (2017) 5743–5753.
[20] C.H. Lorenz, S. Michael, Clinical implications of the osteoprotegerin/RANKL/RANK system for bone and vascular diseases, JAMA 292 (2004) 490–495.
[21] M.K. Saha, P. Agrawal, S.G. Saha, V. Vishwanathan, V. Pathak, Evaluation of correlation between salivary calcium, alkaline phosphatase and osteoporosis- a prospective, comparative and observational study, J. Clin. Diagn. Res. 11 (2017) C63–C66.
[22] Y. Han, G.J. Kim, D. Song, K.H. Chung, K.J. Lee, D.H. Kim, J. An, Calcium supplement derived from Gallus gallus domesticus Promotes BMP-2/RUNX2/SMAD5 and suppresses TRAP/RANK expression through MAPK signaling activation, Nutrients 9 (2017) 504.
[23] T.T. Liu, D.M. Liu, Y. Xuan, L. Zhao, L.H. Sun, D.D. Zhao, X.F. Wang, Y. He, X.Z. Guo, R. Du, The association between the baseline bone resorption marker CTX and incident dysglycemia after 4 years, Bone Res. 5 (2017) 17020.
[24] J. Li, L. Hao, J. Wu, J. Zhang, J. Su, Linarin promotes osteogenic differentiation by activating the BMP-2/RUNX2 pathway via protein kinase A signaling, Int. J. Mol. Med. 37 (2016) 901–910.
[25] L. Min, P. Huang, S. Islam, D.P. Heruth, X. Li, Q.Z. Li, D.Y. Li, Z. Hu, Q.Y. Shui, Epigenetic regulation of Runx2 transcription and osteoblast differentiation by nicotinamide phosphoribosyltransferase, Cell Biosci. 7 (2017) 27.
[26] G. Z, W. S., E K., K. D, Protective effects of melatonin on the activity of SOD, CAT, GSH-Px and GSH content in organs of mice after administration of SNP, Chin. J. Physiol. 60 (2017) 1–10.
[27] H. Sies, Hydrogen peroxide as a central redox signaling molecule in physiological oxidative stress: oxidative eustress, Redox Biol. 11 (2017) 613–619.
[28] H. Lin, X. Gao, G. Chen, J. Sun, J. Chu, K. Jing, P. Li, R. Zeng, B. Wei, Indole-3-carbinol as inhibitors of glucocorticoid-induced apoptosis in osteoblastic cells through blocking ROS-mediated Nrf2 pathway, Biochem. Biophys. Res. Commun. 460 (2015) 422–427.
[29] G. Pellegrini, C. Morales, T. Wallace, L. Plotkin, T. Bellido, Avenanthramides prevent osteoblast and osteocyte apoptosis and induce osteoclast apoptosis in vitro in an Nrf2-independent manner, Nutrients 8 (2016) 423.
[30] P. Hennig, M. Garstkiewicz, S. Grossi, M.D. Filippo, L.E. French, H.D. Beer, The crosstalk between Nrf2 and inflammasomes, Int. J. Mol. Sci. 19 (2018) 562.
[31] Y.X. Sun, L. Lei, K.A. Corry, Z. Pei, Y. Yang, E. Himes, C.L. Mihuti, C. Nelson, G. Dai, J. Li, Deletion of Nrf2 reduces skeletal mechanical properties and decreases load-driven bone formation, Bone 74 (2015) 1–9.
[32] H. Seungha, L. Hyojung, Y. Yoohee, J. Woojin, Nrf2 deficiency induces oxidative stress and promotes RANKL-induced osteoclast differentiation, Free Radic. Biol. Med. 65 (2013) 789–799.
[33] K. Hiroyuki, S. Fumiaki, K. Mikihito, K. Tetsuya, The Keap1/Nrf2 protein axis plays a role in osteoclast differentiation by regulating intracellular reactive oxygen species signaling, J. Biol. Chem. 288 (2013) 23009–23020.